Heliyon 9 (2023) e21134

Contents lists available at ScienceDirect

Heliyon

journal homepage: www.cell.com/heliyon

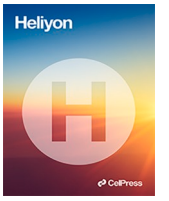

Bassia longifolia (= *Madhuca longifolia*): Isolation of flavan-3-ols and their contribution to the antibacterial and antidiabetic activity in vitro

Peter Bürkel [a], Meena Rajbhandari [b], Guido Jürgenliemk [a,*]

[a] *Department of Pharmaceutical Biology, Universitätsstraße 31, 93053, Regensburg, Germany*
[b] *Research Centre for Applied Science and Technology (RECAST), Kirtipur, Kathmandu, Nepal*

A B S T R A C T

Bassia longifolia KOENIG (= *Madhuca longifolia* (L.) is an evergreen tree that is widely distributed throughout Nepal, India, and Sri Lanka. The bark has various traditional uses: as a paste in the treatment of cuts and wounds or internally as a decoction that is given to diabetic patients. Chemical-analytical and pharmacological investigations regarding the bark are not sufficiently available. We focused on the isolation of flavan-3-ols from the methanolic extract and their contribution to the described traditional uses in wound healing and diabetes treatment. Therefore, an antibacterial assay and an α-glucosidase assay were performed. The isolation process was performed by a combination of Sephadex®-, MCI®-Gel-, and RP-18 chromatography. The structures of the isolated compounds were elucidated by ^{1}H- and ^{13}C-NMR-spectroscopy including COSY, ROESY, HSQC, and HMBC methods. Optical characterization was performed by polarimetry and circular dichroism. Two monomeric, seven dimeric, six trimeric, and one tetrameric flavan-3-ols were found including one dimer and three trimers with rare epiafzelechin units. Two compounds were isolated for the first time. A fraction containing higher oligomeric and polymeric proanthocyanidins (PAs) was examined by ^{13}C NMR spectroscopy and revealed an average degree of polymerization of 8–9. PA with *cis*-configurated subunits predominated at 90 % and the presence of further monohydroxylated flavan-3-ols was revealed. Minimal inhibitory concentrations (MICs) were investigated by the serial microdilution broth assay with *Staphylococcus aureus*. The bacterial suspension was inoculated on agar plates for determining the MICs. The α-glucosidase assay was performed in 96 well plates with α-glucosidase from *Bacillus stearothermophilus*. For the detection of enzyme inhibition, *p*-nitrophenyl-α-D-glucopyranoside was used as a substrate and after incubation absorbance was measured at 405 nm. Antibacterial effects were only found for fractions enriched with PAs or containing higher oligomeric and polymeric flavan-3-ols. All tested substances showed high α-glucosidase inhibition. Whereby 4β→8 conjugated dimers and the monomers showed the lowest inhibition, procyanidin (PC) B5 as 4β→6 conjugated and cinnamtannin A2 as tetrameric flavan-3-ol showed the highest. PAs with epiafzelechin units are rarely found in nature but their reoccurring appearance in *B. longifolia* could be characteristic of this plant. For its traditional uses, the antibacterial activity of the PA-enriched fractions could contribute to the wound healing process when applied to the injured skin. Moreover, all tested substances and fractions showed α-glucosidase inhibition, which could also explain the use of a decoction in the treatment of diabetes. In conclusion, pharmacological investigations could provide scientific evidence for traditional uses of *B. longifolia*.

1. Introduction

In Nepal, traditional phytomedicine has a long history with approximately 1600–1900 different plant species used [1]. One of them is *Bassia longifolia* KOENIG (=*Madhuca longifolia* KOENIG, Sapotaceae), commonly known as the butter tree. It is an evergreen tree that grows about 20 m in height and is distributed throughout Nepal, India, and Sri Lanka. Flowers and bark are used for food and medicine [2,3]. For the food industry, flowers and seeds are of high interest. The flowers are collected and distilled for liquor and to make vinegar [4]. The seeds contain approximately 50 % of fat [5] and therefore are commercially used as mahua butter or mowrah butter.

* Corresponding author.
E-mail address: Guido.Juergenliemk@ur.de (G. Jürgenliemk).

https://doi.org/10.1016/j.heliyon.2023.e21134
Received 17 April 2023; Received in revised form 10 September 2023; Accepted 17 October 2023
Available online 17 October 2023

They have various edible and cosmetical properties [6]. Vernacularly called Mauwa by the indigenous people of Nepal, *B. longifolia* also has various traditional medicinal uses. The flowers are used against coughs, colds, and bronchitis [7]. The bark can be used in different ways: externally as a paste in the treatment of cuts and wounds due to postulated inflammatory properties [8] or internally as a decoction given to diabetic patients [2,3]. Only very few of these indications are investigated pharmacologically and chemically. For example, the ethyl acetate extract of the bark of *B. longifolia* was found to have immunomodulating properties by decreasing T-lymphocyte proliferation and reduction of interleukin-2 secretion in vitro [9]. Furthermore, a methanolic extract of the bark showed antioxidant activity similar to ascorbic acid in a ferric-reducing antioxidant power assay which could indicate a high amount of phenolic compounds [10]. It is important to know more about the plant's chemical compounds to understand its therapeutic effect. Until then, chemical-analytical and spectroscopic investigations are only available for the seeds and showed the presence of oleanane-type triterpene saponins. Data regarding the flowers and bark are not sufficiently available [11,12]. Therefore, a phytochemical characterization of a methanolic extract of the bark of *B. longifolia* is performed for the first time. The total phenolic and tannin content were determined and a fraction containing higher oligomeric and polymeric proanthocyanidins was examined by ^{13}C NMR spectroscopy to characterize its structural properties. In further studies, we evaluated the effect of isolated substances and fractions firstly on the traditional use as a wound healing agent by testing on their antibacterial activity and secondly, the use in the treatment of Diabetes mellitus by testing for inhibition of α-glucosidase.

2. Materials and methods

2.1. Chemicals and reagents

Petroleum ether, ethyl acetate, and methanol (Miller-modification) were obtained by Thermo Fisher Scientific GmbH (Schwerte, Germany). Methanol, acetonitrile (gradient grade for liquid chromatography), formic acid, anisaldehyde, and sulfuric acid were purchased from Merck Chemicals (Darmstadt, Germany). Vanillin was obtained by Carl Roth GmbH + Co. KG (Karlsruhe, Germany). Methanol-d_4 for NMR-spectroscopy was purchased from Sigma Aldrich (Taufkirchen, Germany). Catechin as a reference substance was obtained by PhytoLab GmbH (Vestenbergsgreuth, Germany).

2.2. Plant material

The samples were collected in the Kailali district in western Nepal. The plant was authenticated by Prof. Dr. Sangeeta Rajbhandari, Central Department of Botany, Tribhuvan University. Thereafter, the bark was cut and dried. A voucher specimen (BL-16-DPP) was deposited at the Research Centre for Applied Science and Technology (RECAST), Tribhuvan University, Kathmandu, Nepal.

2.3. Plant extraction

The bark was powdered with a UZM 1 mill (Retsch GmbH, Haan, Germany) with a sieve size of 0.25 mm and yielded 1081.1 g. It was mixed with sea sand (1 + 4) and subsequently percolated with 6.3 L petroleum ether, 17.4 L ethyl acetate, and 17.6 L methanol. After evaporating and lyophilization, 16.73 g petroleum ether, 13.41 g ethyl acetate, and 161.03 g methanol extract were obtained.

2.4. Sephadex® LH-20

The methanolic extract (129.0 g) was fractioned on Sephadex® LH-20 (265.0 g, GE Healthcare GmbH, München, Germany; column: 95 × 3 cm, flow = 0.8–1.2 mL/min) using 70 % ethanol. The column chromatography was controlled by thin layer chromatography (TLC) on silica gel 60 F_{254} (Merck Chemicals GmbH, Darmstadt, Germany; ethyl acetate/formic acid/water 90 + 5+5) with vanillin/HCl and anisaldehyde/H_2SO_4 as detection reagents. Catechin was used as a reference compound in TLC. After the elution of catechin, the mobile phase was changed to 70 % acetone. This yielded a proanthocyanidin enriched fraction (PA-F; 67.99 g). This step was repeated six times and the PA-F fractions of each run were combined and used for further fractionation. PA-F was then again chromatographed on Sephadex® LH-20 column using 70 % ethanol under TLC-control to yield fractions PA 1 (0–1440 mL, 0.29 g), PA 2 (1440-676 mL, 1.24 g), PA 3 (1676–2082 mL, 2.01 g), PA 4 (2082–2280 mL, 1.26 g), PA 5 (2280–2714 mL, 3.46 g), PA 6 (2714–4026 mL, 6.69 g), and PA 7 (4026–4711 mL, 7.18 g). After elution of PA 7, the mobile phase was changed to 70 % acetone to yield Poly-F with polymeric PAs (31.29 g).

2.5. MCI-Gel®

Fractions PA 3-PA 5 were further purified by MCI-Gel® CHP20P (170.0 g, Mitsubishi Chemical Europe GmbH, Düsseldorf, Germany; column: 600 × 25 mm, BESTA-Technik für Chromatographie GmbH, Wilhelmsfeld, Germany) with a Spot Liquid Chromatography Flash machine (Armen Instrument, Paris, France).

System A: A = 20 % methanol, B = 50 % methanol; flow = 7.5 mL/min; gradient: 0–10 min 0 % B, 10–360 min 0 %→100 % B, 360–450 min 100 % B. Subsequently, two isocratic steps of 90 min with 75 % methanol and 100 % methanol were applied. System A was used for PA 3 and yielded the substances **1** (0–1730 mL, 14.60 mg) and **2** (1730–2000 mL, 20.51 mg). System A was also applied to PA4 and yielded substance **5** (3180–3760 mL, 291.4 mg).

System B: Eluents as in system A. Flow = 15 mL/min; gradient: 0–5 min 0 % B, 5–240 min 0 %→100 % B, 240–285 min 100 % B.

Subsequently, two isocratic steps of 45 min with 75 % methanol and 100 % methanol were applied. TLC control in both systems was performed as described in 2.4. System B was used for PA 5 and yielded the fractions PA5 M1 (0–1520 mL, 139.08 mg), PA5 M2 (1520–1827 mL, 213.30 mg), PA5 M3 (1827–2007 mL, 145.48 mg), PA5 M4 (2007–2547 mL, 722.60 mg), PA5 M5 (2547–2760 mL, 136.49 mg), and PA5 M6 (2760–3107 mL, 257.35 mg).

2.6. Preparative HPLC

Binary Agilent Infinity 1260 HPLC equipped with a 1260 Agilent diode array detector, a 1260 Agilent fraction collector, a 1260 Agilent manual injector, and a Nucleodur C18 Isis 5 μm 21.2 × 250 mm column (Macherey-Nagel, Düren, Germany) with guard column and manual injection were used.

Gradient A: A = water, B = methanol; 0–2 min 20 % B isocratic, 2–20 min 20 %→35 % B, 20–21 min 35 %→100 % B, 21–25 min 100 % B, 25–26 min 100 %→20 % B, 26 28 min 20 % B isocratic. Compound **7** eluted at 8.5 min and compound **4** at 10.7 min from PA5 M4.

Gradient B: A = water, B = acetonitrile; 0–2 min 10 % B isocratic, 2–35 min 10 %→18 % B, 35–36 min 18 %→100 % B, 36–40 min 100 % B, 40–41 min 100 %→10 % B, 41–45 min 10 % B isocratic. Compounds **3**, **6**, and **12** eluted at 9.1, 11.2, and 14.1 min from PA5 M2. Compound **11** eluted at 17.1 min from PA5 M3.

Gradient C: A = water, B = acetonitrile; 0–2 min 13 % B isocratic, 2–20 min 13 %→18 % B, 20–21 min 18 %→100 % B, 21–25 min 100 % B, 25–26 min 100 %→ 3 % B, 26–29 min 10 % B isocratic. Compound **8** eluted at 16.1 min, and compound **9** eluted at 17.5 min from PA5 M6. Compounds **10** and **15** were eluted at 12.1 min and 15.0 min from PA5 M5.

Gradient D: A = water, B = acetonitrile; 0–2 min 6 % B isocratic, 2–15 min 6 %→11 % B, 15–16 min 11 %→100 % B, 16–21 min 100 % B, 21–22 min 100 %→6 % B, 22–25 min 6 % B isocratic. Compound **13** eluted at 7.3 min from PA5 M1.

Gradient E: A = water, B = acetonitrile; 0–2 min 12 % B isocratic, 2–35 min 12 %→20 % B, 35–36 min 20 %→100 % B, 36–42 min 100 % B, 42–43 min 100 %→12 % B, 43–48 min 12 % B isocratic. Compound **8** eluted at 16.1 min, and compound **9** eluted at 17.5 min from PA5 M6. Compounds **16** and **14** were eluted at 19.2 min and 28.6 min from PA 6.

2.7. Quantification of phenols and tannins

To quantify the phenols and tannins, the modified method 2.8.14 of the European Pharmacopeia was used [13]. 50.0 mg of powdered bark were suspended and 5.0 mg methanolic extract of *B. longifolia* were dissolved in 1.0 mL water and extracted for 60 min in an ultrasonic bath. Three different dilutions of 2.5 mL/mL, 1.25 mL/mL, and 0.5 mL/mL for the powdered bark extract were made respectively 0.25 mg/mL, 0.125 mg/mL, and 0.05 mg/mL for the methanolic extract. These solutions contain the total phenols. 0.5 mL of this "total phenols solution" (TPS) is subjected to micro-centrifuge tubes (VWR International, Radnor, USA) with 10 mg hide powder (FILK Freiberg Institute GmbH, Freiberg, Germany) and stirred for 60 min without light. This preparation was filtered and represented as the "not adsorbed phenols solution" (NAPS). Either 20 μL TPS or NAPS together with 100 μL Folin-Ciocalteu's reagent (Merck Chemicals GmbH, Darmstadt, Germany) were diluted with 80 μL 10.6 % sodium carbonate solution in a 96-well plate (Greiner Bio-One GmbH, Frickenhausen, Germany). After incubation without light for 180 min, absorbance was measured at 690 nm with a Spectra-FLUOR PLUS® (Tecan Group Ltd., Männedorf, Switzerland). 40.0 mg catechin was dissolved in 100 mL water and used as a reference. All experiments were performed three times and related to the value obtained with the reference using equation (1) to calculate the content of tannins (A = absorbance at 690 nm; m = mass):

$$Content\ of\ tannins\ (\%) = 100 \times \frac{(A_{TPL} - A_{NAPS})_{sample} \times m_{catechin}}{(A_{TPL} - A_{NAPS})_{catechin} \times m_{sample}} \quad (1)$$

2.8. NMR-spectroscopy

The measurements for substances that showed rotational isomerism were performed at 233 K on an AVANCE III HD NMR (Bruker Corporation, Billerica, MA, USA) operating at 400.13 MHz (^{1}H NMR) and 100.63 MHz (^{13}C NMR). The spectra of the structures being accessible to NMR at room temperature (RT) and the screening of the fractions with polymeric proanthocyanidins were measured with an AVANCE III 600 NMR (Bruker Corporation) equipped with a Bruker 5 mm TCI CryoProbe operating at 600.25 MHz (^{1}H NMR) and 150.95 MHz (^{13}C NMR). For structure verification and elucidation, 1D-^{1}H, 1D-^{13}C, [^{1}H–^{13}C]-HSQC, [^{1}H–^{13}C]-HMBC, [^{1}H–^{1}H]-COSY and [^{1}H–^{1}H]-ROESY experiments were performed.

2.9. Mass spectrometry

ESI-HRMS for structure elucidation and verification was performed on a Q-TOF 6540 UHD (Agilent Technologies GmbH, Waldbronn, Germany).

2.10. Circular dichroism

CD-spectra were acquired by a J-715 spectropolarimeter (JASCO Deutschland GmbH, Gross-Umstadt, Germany) operating at 22 °C. The area of measurement was 190–400 nm in 0.5 nm steps with 200 nm/min and 10 cycles. 1 mm Quartz cuvettes (Hellma GmbH &

Co. KG, Müllheim, Germany) were used. All samples were solved in HPLC-grade methanol. The substances were concentrated between 90 and 116 μmol/L. Smoothing the spectra was performed by using the Savitzky-Golay algorithm with a convolution width of 15.

2.11. Polarimetry

The optical rotation values of the isolates were determined using an UniPol L 1000 polarimeter (Schmidt + Haensch GmbH & Co., Berlin, Germany) with a concentration of 0.1 % (0.1 g/100 mL) in HPLC-grade methanol at 589.30 nm (D) and room temperature in a micrometer tube (length: 50 mm; volume: 550 μL). The reported values of the specific rotational angle $[\alpha]_D^{RT}$ were averaged from ten measurements. $[\alpha]_D^{RT}$ is calculated using equation (2) (l = path length in cm; c = concentration, α = rotation angle in deg):

$$[\alpha]_\lambda^T = \frac{\alpha}{c \times l} \text{ indeg xcm}^2 \text{ x g}^{-1} \quad (2)$$

2.12. Serial microdilution broth assay

Minimal inhibitory concentrations (MICs) were investigated by the serial microdilution broth assay according to EUCAST protocols with *Staphylococcus aureus* (ATCC 12600; German Collection of Microorganisms and Cell cultures GmbH, Braunschweig, Germany) cultivated in LB-broth (Miller-modification; Thermo Fisher Scientific GmbH, Schwerte, Germany). Bacteria suspension was diluted to 10^8 colony-forming units (CFU)/mL. Samples were dissolved in DMSO. For the methanolic extract, the PA enriched fraction (PA-F), and fraction Poly-F, a serial two-fold microdilution was performed in a concentration range of 5.00-0.16 mg/mL in a 96-well plate (Greiner Bio-One GmbH, Frickenhausen, Germany). A concentration range of 512-64 μM was used for the isolates. Each well contained 50 μL LB-medium, 100 μL bacteria suspension, and either 50 μL sample, 50 μL DMSO (negative control) or 50 μL DMSO and 10 μL 3 mg/mL chloramphenicol (Sigma Aldrich, Taufkirchen, Germany) dissolved in 70 % ethanol (positive control). Microdilution plates were incubated at 37 °C for 24 h and then subcultivated by inoculating 10 μL of every sample dilution and controls on the surface of agar plates (VWR International GmbH, Darmstadt, Germany) and incubated for another 24 h at 37 °C. MIC was defined as the lowest concentration of sample that allows no visible growth of bacteria. The assay was performed three times for each sample.

2.13. α-glucosidase assay

The basic principle of the assay is the cleavage of the α-glucose of *p*-nitrophenyl-α-D-glucopyranoside (*p*NPG) by α-glucosidase (both Sigma Aldrich, Taufkirchen, Germany), resulting in the yellow *p*-nitrophenol. For the assay α-glucosidase from *Bacillus stearothermophilus* was used. In each well of a 96-well plate 70 μL 0,1 M phosphate buffer (pH = 6.8), 10 μL 0,4 U/mL α-glucosidase, and either 10 μL sample (concentration range in wells: 32-1 μM for the isolates and 4–0.25 μg/mL for the fractions in deionized water), 10 μL deionized water (negative control) or 10 μL 1,28 mM acarbose in buffer (positive control) were added. After the addition of 10 μL of 10 mM *p*NPG, the 96-well plates were immediately incubated for 20 min at 60 °C. After incubation and the addition of 150 μL 2 M Na_2CO_3 solution to stop enzyme activity, the absorbance was measured at 405 nm in a SpectraFLUOR PLUS® (Tecan Group Ltd., Männedorf, Switzerland). The assay was performed three times in tetraplicates for each sample. Determining of IC_{50} values and statistical analyses were performed with GraphPad Prism 9 (San Diego, USA).

3. Results and discussion

3.1. Isolation and structure elucidation

A methanolic extract obtained from the bark of *B. longifolia* was used for the isolation of flavan-3-ols. After several runs using Sephadex®-LH20 to gain the flavan-3-ol enriched fraction (PA-F), a second chromatography on Sephadex®-LH20 with the combined PA-F was performed, to gain the fractions PA1-Poly-F. Fractionation of PA 3 on MCI®-gel with system A yielded the fractions PA3 M1 and PA3 M2 that could be identified as the monomers (+)-catechin and (−)-epicatechin (**1**, **2**). Further fractionation of PA 4 with system A led to the fraction PA4 M2 which consisted of epiafzelechin-(4β→8)-epicatechin (**5**). MCI®-gel-fractionation system B was used for PA 5 and yielded the fractions PA5 M1-PA5 M8. Final purification of PA5 M1-PA5 M6 with preparative HPLC on an RP-18 column yielded the compounds **3**, **4** and **6**–**13** as well as the substances **14** and **16** from PA 6.

The structures of the compounds (**1**-**16**) were confirmed by performing ^1H, ^{13}C NMR spectroscopy as well as the heteronuclear 2D-NMR-experiments HSQC, HMBC, and homonuclear COSY and ROESY. The measurements were conducted at 233 K for oligomeric flavan-3-ols with complete or partial 4β→8 configuration (**3**–**5, 8**–**13, 16**) to avoid rotational isomerism and at room temperature for the 4α (**6, 7, 15**) or 4β→6 linked dimers (**14**). Mass was received by HR-ESI-MS in negative mode. The structures of compounds **1**–**7, 10, 12, 14,** and **16** were confirmed by comparing the NMR-spectroscopic data of the substances with the literature [14–20]. For substances **8** and **13**, only data for the peracetylated compound can be found in the literature [21,22]. Compounds **9** and **11** are described here for the first time.

CD spectroscopy is the proven method of choice to verify the 4α or 4β linkage between the flavan-3-ol units. High-amplitude positive Cotton effects at low wavelengths (220–240 nm) indicate a 4β- and negative Cotton effects a 4α-configuration [23,24]. PC B3 (**6**, CD-spectrum displayed in supplementary data) shows a CD-spectrum that would rather indicate a 4β-configuration which might be caused by impurities as all other spectroscopic data are in excellent accordance with literature data [16,25,26].

In PA structure analysis, the proof of the interflavanoid linkage has always been a much-discussed topic [27]. To validate the structure of the 4*α*→6 linked PA procyanidin B8 (**15**), extensive literature research was performed. Comparing the NMR data for the free phenolic compound, the literature itself showed differences among each other and was only partially in accordance with the measured shifts [28,29]. Therefore, a different way of proving the structure had to be found. A characteristic multiplet (m) at 4.17 ppm for H–3_C and a doublet (d) at 5.03 ppm for H–2_C revealed a 3,4-*trans*-configuration of the upper unit. The *cis*-configuration of the lower unit was proven due to a typical broad singlet (br s) at 4.04 ppm for H–3_F and a singlet at 4.73 ppm for H–2_F. These shifts and signals for the subunits were in perfect accordance with the other isolated substances. For catechin as the upper, epicatechin as the lower unit, and with the according sum formula given by MS experiments, now only PC B4 (4*α*→8 linkage) or PC B8 (4*α*→6 linkage) were possible molecules. PC B4 was already isolated at this point and its structure was confirmed unambiguously due to different references [30,31]. The intermolecular linkage could be determined from the presence or absence of specific signals in the 2D phase-sensitive ROESY. Substances with 4 → 8 configuration showed cross signals between H–3_C/H–4_C of the upper unit and H-$2'_E$/H-$6'_E$ of the lower unit due to its spatial proximity while 4 → 6 configurated dimers lack these signals (Fig. 3). The ROESY-spectra with the discussed cross signals are displayed in the supplementary material. The negative Cotton-effect between 205 and 240 nm proved the 4α→6 linkage eventually (Fig. 2). Due to the findings in these experiments, the structure of PC B8 (**15**) was proven conclusively.

For the two new structures **9** and **11**, the structure elucidation is described exemplarily for substance **11**. *Cis*-configuration of the top unit was identified by a characteristic doublet (d) with a small coupling constant of $J_{H\text{-}2/H\text{-}3} = 1.4$ Hz at 3.75 ppm for H–3_C and a singlet (s) at 5.41 ppm for H–2_C. *Trans*-configuration in the middle unit was confirmed by a typical m at 4.34 pp for H–3_F, a d for H–2_F,

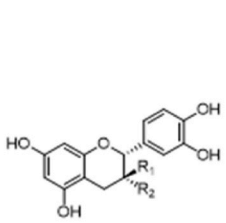

1: (+)-catechin; R_1 = OH, R_2 = H

2: (-)-epicatechin; R_1 = H, R_2 = OH

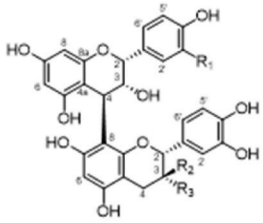

3: PC B1; R_1 = OH, R_2 = OH; R_3 = H
4: PC B2; R_1 = OH, R_2 = H; R_3 = OH
5: epiafzelechin-(4*β*→8)-epicatechin; R_1 = H, R_2 = H, R_3 = OH

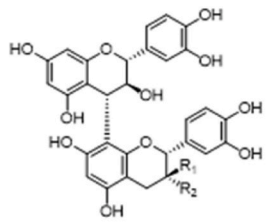

6: PC B3; R_1 = OH, R_2 = H

7: PC B4; R_1 = H, R_2 = OH

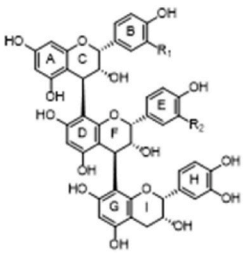

8: epiafzelechin-(4*β*→8)-epicatechin-(4*β*→8)-epicatechin; R_1 = H, R_2 = OH
9: epicatechin-(4*β*→8)-epiafzelechin-(4*β*→8)-epicatechin; R_1 = OH, R_2 = H
10:PC C1; R_1 = OH, R_2 = OH

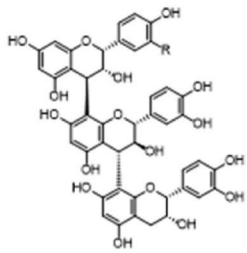

11:epiafzelechin-(4*β*→8)-catechin-(4*α*→8)-epicatechin; R = H

12: epicatechin-(4*β*→8)-catechin-(4*α*→8)-epicatechin; R = OH

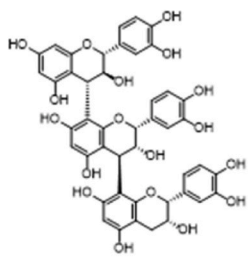

13: catechin-(4*α*→8)-epicatechin-(4*β*→8)-epicatechin

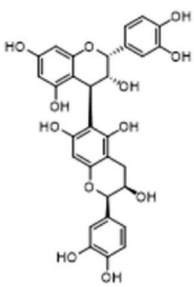

14: PC B5

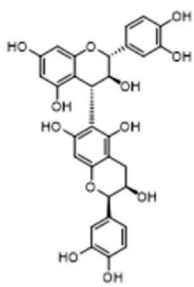

15: PC B8

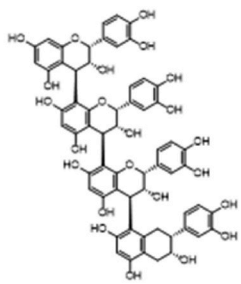

16: cinnamtannin A2

Fig. 1. Structures of the isolated flavan-3-ols **1**–**16**.

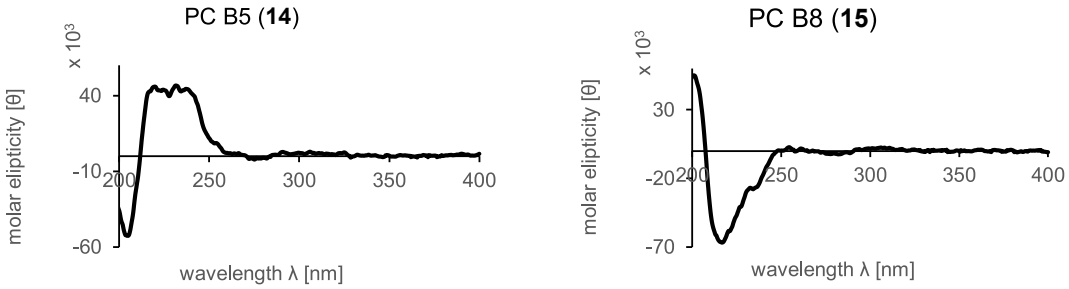

Fig. 2. CD-spectra of 4β→6 linked PC B5 with a positive cotton effect and 4α →6 linked PC B8 with a negative cotton effect (295 K, MeOH).

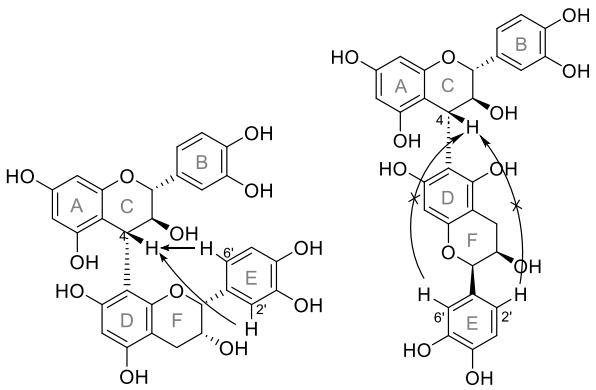

Fig. 3. ROESY signals for PC B4 (**A**, **7**) that verify a 4 → 8 linkage and PC B8 (**B**, **15**) that lack these signals.

and the associated ^{13}C shift at 83.5 ppm. Typical for a *cis*-configurated bottom unit, a broad s for H–3$_I$ at 4.21 ppm and an s for H–2$_I$ at 4.93 ppm is observed which can also be found in the NMR spectrum of the monomer epicatechin. The monohydroxylated B-ring of epiafzelechin as the top unit was established by a d at 7.30 ppm for H-2′$_B$ and H-6′$_B$ and an m at 6.75 ppm for H-3′$_B$ and H-5′$_B$. Both integrated for two protons and therefore indicated an AA'BB′-spin system of the B-ring. A correlation between the d at 7.30 ppm for H-2′$_B$ and H-6′$_B$ with the signal at 76.7 ppm from H–2$_C$ in the top unit was observed in the HMBC spectrum. Further HMBC correlations are given in Fig. 4. The ROESY-spectrum showed the characteristic cross signals between H–3$_{C/F}$/H–4$_{C/F}$ of the upper and middle unit and

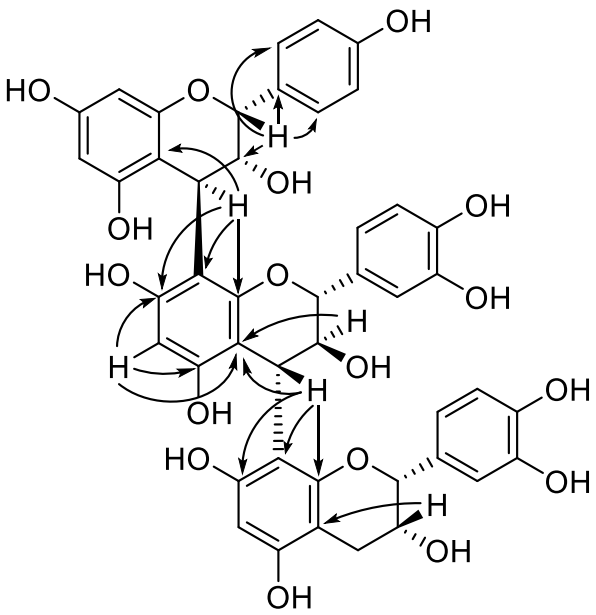

Fig. 4. Key HMBC correlations for compound **11**.

H-2′$_{E/H}$/H-6′$_{E/H}$ of the middle and lower unit. These signals clearly indicate C-4 to C-8 linkages. The CD-spectrum (supplementary data) showed a negative Cotton-effect between 205 and 233 nm which is caused by the 4α-linkage between the middle and the lower unit. For all isolated substances, a 2-3-*cis*-configurated unit was always followed by a 4β-configuration with the lower unit, which is also confirmed by almost every isolation study which is found in the literature. Therefore, a 4β-configuration between the upper and the middle unit is postulated which leads to the structure of compound **11** as epiafzelechin-(4β→8)-catechin-(4α→8)-epicatechin.

3.2. Total phenolic and tannin content

The most common principle for the quantification of phenols and tannins is the Folin-Ciocalteu's reagent method described in the European Pharmacopeia's method 2.8.14 [32]. Phenols reduce phosphotungstic acid in the Folin-Ciocalteu's reagent to blue tungsten oxides with a broad absorption maximum at 580–820 nm [33]. Therefore, any reducing substance reacts with the reagent e.g. other phenolic compounds like flavonoids or phenylpropanoids. In this work, a modified method developed by Wiesneth et al. [13] for a higher sample throughput was used. Both, the methanolic extract and the whole bark of *B. longifolia* were investigated. The results can be found in Table 1.

Due to many different methods for the quantification of phenols and tannins, only data that were obtained with the same method can be used to compare the content of phenols and tannins among other species. In previous investigations, the content of phenols and tannins for different *Salix* species during one growing season in leaves and sprouts was determined. The highest content of phenols was found to be between 4 and 8% and the highest content of tannins was between 2 and 8% [34]. For the bark of *Quercus robur*, which is used because of its "high" tannin content in Traditional European Medicine, a content of 5.1 % phenols and 4.3 % tannins was determined [13,33]. This indicates a comparatively high amount of phenols and tannins in the bark of *B. longifolia*. Furthermore, the content of tannins is as high as the content of phenols which indicates that almost all phenolic compounds consist of tannins.

3.3. Characterization of a fraction with polymeric proanthocyanidins with ^{13}C NMR

Coloumn-chromatography with Sephadex® LH-20 yielded the fractions PA 1-Poly-F. PA1-PA7 were eluted with ethanol 70 % and contain monomeric (PA 3, PA 4), dimeric (PA 4, PA 5, PA 6), trimeric (PA 5), tetrameric (PA 6), and higher oligomeric PAs (PA 6, PA 7). After eluting these compounds, the eluent was changed to acetone 70 % to yield the polymeric flavan-3-ols (Poly-F.). Although isolation and structure elucidation of oligomeric proanthocyanidins higher than tetrameric flavan-3-ols is challenging concerning their full stereochemistry, a lot of structural information about the flavan-3-ol composition of higher oligomers can be obtained by ^{13}C NMR spectroscopy and calculating the ratio of distinct carbon signals [35].

The average degree of polymerization (DP) can be estimated by the integration of the C-4 signals of extender units (N, δ_C = 36–39 ppm) and the integration of C-4 signals of the terminal units (O, δ_C = 29–31 ppm; [16]. A second way to calculate the DP is to integrate the C-3 resonances of the extender (L, δ_C = 71–74 ppm) and terminal units (M, δ_C = 66–68 ppm; [36]. With both methods, an average degree of polymerization of 8–9 could be estimated. ^{13}C NMR spectroscopy makes it also possible to get stereochemical information about the relative configuration of the flavan-3-ol units on C-2 and C-3. The signal from 76 to 78 ppm (K_2, Fig. 6) can be assigned to the *cis*-configurated C-2 of the extender units, and the signal from 79 to 80 ppm (K_1, Fig. 6) to the *cis*-configurated C-2 of the terminal units. The signal cluster at 82–85 ppm (J, Fig. 6) can be assigned to the *trans*-configurated C-2 of both, the terminal and extender units. The amount of *cis*-configurated flavan-3-ols in the polymeric fraction is more than 90 %. Moreover, characteristic signals at 128–130 ppm (D, Fig. 5) are caused by C-2′ and C-6′ in monohydroxylated B-rings as they occur in proanthocyanidins with (epi)afzelechin units. This is in accordance with the results of the present work as four compounds with epiafzelechin units (**5, 8, 9, 11**, Fig. 1) could have been isolated. Signals at 108–109 ppm would be induced by C-2′ and C-6' of trihydroxylated B-rings as in (epi)gallocatechin units but could not be found in the polymeric fraction *of B. longifolia* as well as in the isolation process. The lack of typical sugar signals (δ_C = 62–76 ppm) indicates their absence as well as the absence of carbonyl- or carboxyl carbons at ca. δ_C = 200 ppm and 170 ppm, respectively, indicating that there is no acyl substitution in the set of polymers.

3.4. Antibacterial activity

B. longifolia is described as possessing wound-healing properties. In a previous study, a wound-healing assay was performed by Zimmermann-Klemd et al. [9] which showed no effect though. Therefore, we tested antibacterial activity as a possible assisting effect in wound healing. As bacterium *S. aureus* was chosen, as it naturally populates human skin [37]. In traditional use, the extract is put directly on the injured skin, so we decided to test comparatively high doses up to 5 mg/mL for the extract and fractions. In a serial microdilution broth assay, all of the isolated substances as well as the methanolic extract, the PA enriched fraction (PA-F.), and fraction

Table 1
Determination of the total phenolic and tannin content. All values were calculated as catechin and results are depicted in % [m/m] ± standard deviation (n = 3).

	methanolic extract	bark extract
phenols ± SD [%]	43.1 ± 1.4	9.9 ± 0.9
tannins ± SD [%]	42.2 ± 2.0	9.9 ± 1.0

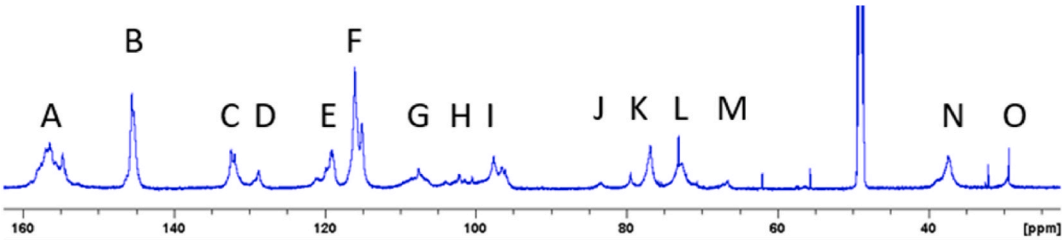

Fig. 5. ^{13}C NMR spectrum of Poly-F. (150 MHz, MeOH-d_4, 293 K, 205 mg). (**A**) C-5/C-7/C-8a of A-rings; (**B**) C-3'/C-4′ of procyanidin units; (**C**) C-1′ of B-rings; (**D**) C-2'/C-6′ of monohydroxylated B-rings; (**E-F**) C-2'/C-5'/C-6′ of PC units; (**G**) substituted A-ring carbons; (**H**) C-4a of PC units; (**I**) C-6/C-8 of A-rings; (**J**) C-2 of 2,3- *trans* units; (**K**) C-2 of 2,3-*cis* units; (**L**) C-3 of extender units; (**M**) C-3 of terminal units, (**N**) C-4 of upper and middle (extender) units, (**O**) C-4 of terminal units.

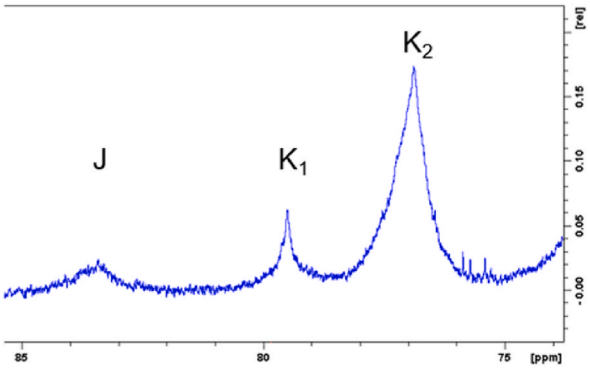

Fig. 6. Signals of C-2 of *cis*- and *trans*-configurated flavan-3-ols.

Poly-F. with polymeric PAs were tested. Neither the tested substances nor the methanolic extract showed an inhibitory effect on bacterial growth. Only PA-F. and Poly-F. showed antibacterial effects in the tested concentration range. PA-F. and Poly-F. revealed a MIC of 4.2 ± 1.2 mg/mL and 3.3 ± 1.2 mg/mL. These results indicate that only a mixture of PAs has an antibacterial effect and also that a higher concentration of polymeric PAs might have a stronger effect.

3.5. *α-glucosidase inhibition*

In the human body, α-glucosidases are responsible for the digestion of small oligosaccharides and disaccharides into monosaccharides which then leads to a rise in blood glucose levels [38,39]. The enzyme used in this assay was isolated from *B. stearothermophilus* which is highly specific for α-1,4-glucosidic bonds of maltooligosaccharides [40]. In this study, the isolated substances, as well as Poly-F, PA-F and the methanolic extract were tested for their capacity to inhibit the enzyme. Acarbose, a well-known inhibitor was also tested and used as a positive control. Acarbose showed the strongest inhibition of all tested substances (IC_{50} = 2.9 ± 0.4 nM). For the three fractions, Poly-F. with polymeric flavan-3-ols showed the lowest IC_{50} value (3.2 ± 1.6 μg/mL) followed by PA-F. (IC_{50} = 4.0 ± 0.8 μg/mL) and the methanolic extract (IC_{50} = 7.8 ± 1.6 μg/mL). Again, the highest inhibitory effect is observed in the fraction with the highest amount of polymeric PAs (Poly-F) and in a PA-enriched fraction (PA-F.) whereas the methanolic extract shows comparatively the lowest inhibition.

The determined IC_{50} values for the isolated compounds are displayed in Table 2.

Unfortunately, the yield for PC B8 (**15**) was too low to be tested. Every tested substance showed high inhibition of α-glucosidase. Within these compounds, the very common monomeric flavan-3-ols catechin (**1**) and epicatechin (**2**) and the 4β→8 linked dimers PC B1 (**3**) and PC B2 (**4**) showed the lowest inhibition. The lowest IC_{50} values and therefore highest inhibition of α-glucosidase were observed for the tetrameric cinnamtannin A2 (**16**) and PC B5 (**14**). This study was aimed to determine a structure-activity relationship between PAs and α-glucosidase-inhibition. For the tested fractions, the effect increased with the concentration of PAs and the DP. The monomers (**1**, **2**) and the 4β→8 configurated dimers (**3**, **4**, **5**) showed the lowest and cinnamtannin A2 (**16**) and PC B5 (**14**) the highest inhibition. The pharmacological effect seems to be dependent on the DP and the intermolecular linkage. Flavan-3-ols with a 4α-linkage (**6**, **7**, **11**–**13**) and trimeric and tetrameric PAs showed better inhibition than 4β→8 configurated substances or dimers (Fig. 7).

4. Conclusions

In the present study, a phytochemical characterization of *B. longifolia* was performed for the first time in which 16 different flavan-3-ols were found. Literature research for proanthocyanidins with different databases like SciFinder® or PubMed® (January 18, 2022)

Table 2
IC_{50}±SD [μM] values of the isolated compounds (n = 3).

monomers	IC_{50}	dimers	IC_{50}	trimers	IC_{50}	tetramers	IC_{50}
1	8.4 ± 1.1	**3**	11.2 ± 1.0	**8**	8.6 ± 1.5	**16**	1.7 ± 0.1
2	8.5 ± 0.9	**4**	8.5 ± 1.5	**9**	6.3 ± 0.6		
		5	2.3 ± 0.8	**10**	3.4 ± 1.1		
		6	2.4 ± 0.3	**11**	4.5 ± 0.7		
		7	3.0 ± 0.5	**12**	5.3 ± 0.5		
		14	1.6 ± 0.4	**13**	2.2 ± 0.1		

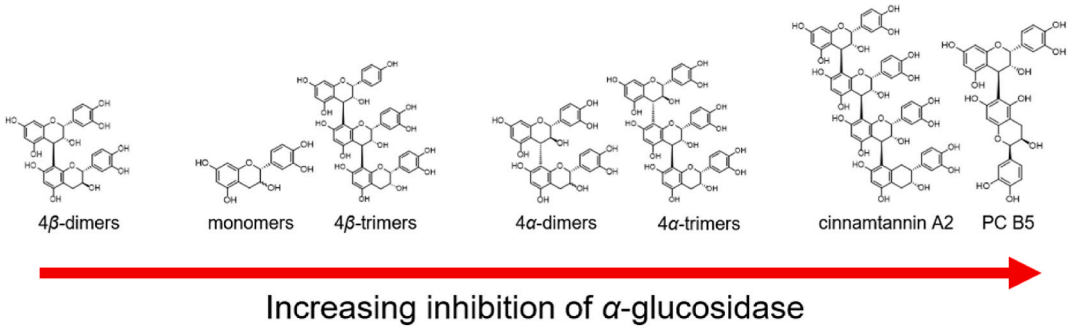

Fig. 7. Structures of some tested compounds concerning α-glucosidase inhibition.

shows only very few results for studies with monohydroxylated flavan-3-ols in comparison to di- or trihydroxylated flavan-3-ols. This leads to the assumption that these compounds are rarely distributed in the plant kingdom. Although the monomeric (epi)afzelechin could not be found in the present study, one dimer (**5**) with a very high yield and three trimers with epiafzelechin units (**8**, **9**, **11**) were isolated. Therefore, *B. longifolia* as a new source for these rare proanthocyanidins could be established. For the traditional use in wound healing, an antibacterial effect against *S. aureus* was found for the PA-enriched fractions PA-F and Poly-F, indicating that a higher DP leads to a stronger effect. This could play an assisting role in the wound-healing process. As an application as a decoction for diabetic patients, the effect on α-glucosidase was investigated. The results show a strong inhibition for the isolated compounds as well as for the extract and fractions. Tetrameric cinnamtannin A2 (**16**), the 4α-configurated compounds (**6**, **7**, **11**–**13**), and PC B5 (**14**) showed the highest inhibition whereas the monomers (**1**, **2**) and the 4β-configurated dimers (**3**, **4**, **5**) showed the lowest. For both assays, an increase in the amount of higher oligomeric fractions led to a stronger pharmacological effect. Although a tendency is apparent, no general statement about a structure-activity relationship for flavan-3-ols in general can be made. For the traditional use of the bark of *B. longifolia*, the first evidence as an antidiabetic drug is given in this study. Although *B. longifolia* has various traditional and commercial uses, almost no studies about their constituents and pharmacological evidence were performed. In this work, the first step to close this gap was done.

Author contribution statement

Peter Bürkel: Conceived and designed the experiments; Performed the experiments; Analyzed and interpreted the data; Contributed reagents, materials, analysis tools or data; Wrote the paper.

Meena Rajbhandari: Contributed reagents, materials, analysis tools or data.

Guido Jürgenliemk: Conceived and designed the experiments; Contributed reagents, materials, analysis tools or data.

Data availability statement

Data included in article/supp. material/referenced in article.

Declaration of competing interest

The authors declare that they have no known competing financial interests or personal relationships that could have appeared to influence the work reported in this paper.

Acknowledgments

Many thanks are due to Prof. J. Heilmann (University of Regensburg, Germany) for helpful discussions, Professor S. Rajbhandari

(Tribhuvan University, Kathmandu, Nepal) for authenticating the plant, and Mr. D. P. Paneru and S. Bam for sample collection. T.-A. Nguyen, F. Kastner, and J. Kiermaier for the recording of NMR- and MS-spectra and A. Dürkop for generating the CD spectra are thankfully acknowledged (all analytical department, Faculty of Chemistry and Pharmacy, University of Regensburg, Germany).

List of Abbreviations

CD	circular dichroism
NAPS	not absorbed phenols solution
CFU	colony forming units
PA	proanthocyanidin
COESY	correlated Spectroscopy
PA-F.	proanthocyanidin-fraction
d	doublet
PC	procyanidin
DP	degree of polymerization
Poly-F.	polymeric fraction
ESI	electrospray ionization
*p*NPG	*p*-nitrophenyl-α-D-glucopyranoside
HMBC	heteronuclear multiple bond correlation
ROESY	rotating-frame nuclear overhauser effect correlation spectroscopy
HPLC	high-pressure liquid chromatography
RP	reversed-phase
HRMS	high-resolution mass spectrometry
RT	room temperature
HSQC	heteronuclear single quantum coherence
s	singlett
IC	inhibitory concentration
SD	standard deviation
m	multiplett
TOF	time of flight
MIC	minimal inhibitory concentration
TPS	total phenols solution

List of compounds studied

(+)-catechin	procyanidin C1
(−)-epicatechin	epiafzelechin-(4β→8)-epicatechin
procyanidin B1	epiafzelechin-(4β→8)-epicatechin-(4β→8)-epicatechin
procyanidin B2	epicatechin-(4β→8)-epiafzelechin-(4β→8)-epicatechin
procyanidin B3	epiafzelechin-(4β→8)-catechin-(4α→8)-epicatechin
procyanidin B4	epicatechin-(4β→8)-catechin-(4α→8)-epicatechin
procyanidin B5	catechin-(4α→8)-epicatechin-(4β→8)-epicatechin
procyanidin B8	cinnamtannin A2

Appendix A. Supplementary data

Supplementary data to this article can be found online at https://doi.org/10.1016/j.heliyon.2023.e21134.

References

[1] B.P. Gaire, L. Subedi, Medicinal plant diversity and their pharmacological aspects of Nepal himalayas, Phcog. J. 3 (2011) 6–17, https://doi.org/10.5530/pj.2011.25.2.
[2] N.P. Manandhar, S. Manandhar, Plants and People of Nepal, Timber Press, Portland, OR, 2002.
[3] K.N. Akshatha, S. Mahadeva Murthy, N. Lakshmidevi, Ethnomedical uses of Madhuca longifolia-a review, International Journal of Life Science & Pharma Research (2013) 44–53.
[4] M.F. Ramadan, A.A.A. Mohdaly, A.M.A. Assiri, M. Tadros, B. Niemeyer, Functional characteristics, nutritional value and industrial applications of Madhuca longifolia seeds: an overview, J. Food Sci. Technol. 53 (2016) 2149–2157, https://doi.org/10.1007/s13197-015-2095-6.
[5] A. Singh, I.S. Singh, Chemical evaluation of mahua (Madhuca indica) seed, Food Chem. 40 (1991) 221–228, https://doi.org/10.1016/0308-8146(91)90106-X.
[6] Mohamed Fawzy, Ramadan Hassanien, Mahua Butter: Nature's Novel Fat, Unpublished, 2011.
[7] M.B. Rai, Medicinal plants of tehrathum district, eastern Nepal, Our Nat. 1 (2006) 42–48, https://doi.org/10.3126/on.v1i1.304.

[8] A.G. Singh, J.P. Hamal, Traditional phytotherapy of some medicinal plants used by tharu and Magar communities of western Nepal, against dermatological disorders, Sci. World 11 (2013) 81–89, https://doi.org/10.3126/sw.v11i11.8558.

[9] A.M. Zimmermann-Klemd, V. Konradi, C. Steinborn, A. Ücker, C.M. Falanga, U. Woelfle, R. Huber, G. Jürgenliemk, M. Rajbhandari, C. Gründemann, Influence of traditionally used Nepalese plants on wound healing and immunological properties using primary human cells in vitro, J. Ethnopharmacol. 235 (2019) 415–423, https://doi.org/10.1016/j.jep.2019.02.034.

[10] A.P. Dahake, Chiranatan Chakma, Deshbandhu Joshi, Rita Chakma, Alok Tripathi, Antioxidant activity of methanolic extract of Madhuca longifolia bark, J. Pharm. Res. (2010) 1709–1711.

[11] K. Yoshikawa, M. Tanaka, S. Arihara, B.C. Pal, S.K. Roy, E. Matsumura, S. Katayama, New oleanene triterpenoid saponins from madhucalongifolia, J. Nat. Prod. 63 (2000) 1679–1681, https://doi.org/10.1021/np000351r.

[12] I. Kitagawa, A. Inada, I. Yosioka, Saponin and sapogenol. Xii. Mi-saponin A and mi-saponin B, two major bisdesmosides from the seed kernels of Madhuca longifolia (L.), MACBRIDE. Chem. Pharm. Bull. 23 (1975) 2268–2278, https://doi.org/10.1248/cpb.23.2268.

[13] S. Wiesneth, G. Jürgenliemk, Total phenolic and tannins determination: a modification of Ph. Eur. 2.8.14 for higher throughput, Pharmazie 72 (2017) 195–196, https://doi.org/10.1691/ph.2017.6911.

[14] R. Seto, H. Nakamura, F. Nanjo, Y. Hara, Preparation of epimers of tea catechins by heat treatment, Biosci., Biotechnol., Biochem. 61 (1997) 1434–1439, https://doi.org/10.1271/bbb.61.1434.

[15] A.L. Davis, Y. Cai, A.P. Davies, J.R. Lewis, 1H and13C NMR assignments of some green tea polyphenols, Magn. Reson. Chem. 34 (1996) 887–890, https://doi.org/10.1002/(SICI)1097-458X, 199611)34:11<887::AID-OMR995>3.0.CO;2-U.

[16] S. Wiesneth, F. Petereit, G. Jürgenliemk, Salix daphnoides: a screening for oligomeric and polymeric proanthocyanidins, Molecules 20 (2015) 13764–13779, https://doi.org/10.3390/molecules200813764.

[17] A. Alejo-Armijo, A. Tello-Abolafia, S. Salido, J. Altarejos, Phenolic compounds in Laurel Wood: a new source of proanthocyanidins, J. Wood Chem. Technol. 39 (2019) 436–453, https://doi.org/10.1080/02773813.2019.1636825.

[18] J. Lokvam, T.A. Kursar, Divergence in structure and activity of phenolic defenses in young leaves of two co-occurring Inga species, J. Chem. Ecol. 31 (2005) 2563–2580, https://doi.org/10.1007/s10886-005-7614-x.

[19] H. Kolodziej, Synthesis and characterization of procyanidin dimers as their peracetates and octamethyl ether diacetates, Phytochemistry 25 (1986) 1209–1215, https://doi.org/10.1016/S0031-9422(00)81582-4.

[20] T. Shoji, M. Mutsuga, T. Nakamura, T. Kanda, H. Akiyama, Y. Goda, Isolation and structural elucidation of some procyanidins from apple by low-temperature nuclear magnetic resonance, J. Agric. Food Chem. 51 (2003) 3806–3813, https://doi.org/10.1021/jf0300184.

[21] J. Bicker, F. Petereit, A. Hensel, Proanthocyanidins and a phloroglucinol derivative from Rumex acetosa L, Fitoterapia 80 (2009) 483–495, https://doi.org/10.1016/j.fitote.2009.08.015.

[22] H. Kolodziej, Oligomeric flavan-3-ols from medicinal willow bark, Phytochemistry 29 (1990) 955–960, https://doi.org/10.1016/0031-9422(90)80054-K.

[23] M.W. Barrett, W. Klyne, P.M. Scopes, A.C. Fletcher, L.J. Porter, E. Haslam, Plant proanthocyanidins. Part 6. Chiroptical studies. Part 95. Circular dichroism of procyanidins, J. Chem. Soc., Perkin Trans. 1 (1979) 2375, https://doi.org/10.1039/p19790002375.

[24] J.J. Botha, D.A. Young, D. Ferreira, D.G. Roux, Synthesis of condensed tannins. Part 1. Stereoselective and stereospecific syntheses of optically pure 4-arylflavan-3-ols, and assessment of their absolute stereochemistry at C-4 by means of circular dichroism, J. Chem. Soc., Perkin Trans. 1 (1981) 1213, https://doi.org/10.1039/p19810001213.

[25] H. Makabe, T. Kamo, M. Hirota, Y. Mohri, M. Sagehashi, T. Yamada, Y. Hattori, K. Morimura, An efficient synthesis of procyanidins using equimolar condensation of catechin and/or epicatechin catalyzed by ytterbium triflate, HETEROCYCLES 79 (2009) 549, https://doi.org/10.3987/COM-08-S(D)14.

[26] C.J. Hayes, B.P. Whittaker, S.A. Watson, A.M. Grabowska, Synthesis and preliminary anticancer activity studies of C4 and C8-modified derivatives of catechin gallate (CG) and epicatechin gallate (ECG), J. Org. Chem. 71 (2006) 9701–9712, https://doi.org/10.1021/jo061740e.

[27] L. Balas, J. Vercauteren, Extensive high-resolution reverse 2D NMR analysis for the structural elucidation of procyanidin oligomers, Magn. Reson. Chem. 32 (1994) 386–393, https://doi.org/10.1002/mrc.1260320703.

[28] T de Bruyne, L. Pieters, R. Dommisse, H. Kolodziej, V. Wray, D. Vanden Berghe, A. Vlietinck, NMR characterization and biological evaluation of proanthocyanidins: a systematic approach, Basic Life Sci. 66 (1999) 193–209, https://doi.org/10.1007/978-1-4615-4139-4_10.

[29] T. Esatbeyoglu, V. Wray, P. Winterhalter, Dimeric procyanidins: screening for B1 to B8 and semisynthetic preparation of B3, B4, B6, and B8 from a polymeric procyanidin fraction of white willow bark (Salix alba), J. Agric. Food Chem. 58 (2010) 7820–7830, https://doi.org/10.1021/jf101023e.

[30] N. Nakajima, A. Saito, A. Tanaka, M. Ubukata, Synthetic studies of proanthocyanidins. Part 4. The synthesis of procyanidin B1 and B4: TMSOTf-catalyzed cyclization of catechin and epicatechin condensation, HETEROCYCLES 61 (2003) 287, https://doi.org/10.3987/COM-03-S37.

[31] Y. Mohri, M. Sagehashi, T. Yamada, Y. Hattori, K. Morimura, T. Kamo, M. Hirota, H. Makabe, An efficient synthesis of procyanidins. Rare earth metal Lewis acid catalyzed equimolar condensation of catechin and epicatechin, Tetrahedron Lett. 48 (2007) 5891–5894, https://doi.org/10.1016/j.tetlet.2007.06.047.

[32] Bundesinstitut für Arzneimittel und Medizinprodukte, in: Europäisches Arzneibuch 10.0: 2.8.14 Gerbstoffe in Pflanzlichen Drogen vol. 10, Deutscher Apotheker Verlag, Stuttgart, Germany, 2020.

[33] O. Sticher, J. Heilmann, I. Zündorf, R. Hänsel, Hänsel/Sticher, Pharmakognosie Phytopharmazie, tenth ed., Wissenschaftliche Verlagsgesellschaft, Stuttgart, 2015.

[34] S. Wiesneth, G. Aas, J. Heilmann, G. Jürgenliemk, Investigation of the flavan-3-ol patterns in willow species during one growing-season, Phytochemistry 145 (2018) 26–39, https://doi.org/10.1016/j.phytochem.2017.10.001.

[35] R.H. Newman, L.J. Porter, L.Y. Foo, S.R. Johns, R.I. Willing, High-resolution13C NMR studies of proanthocyanidin polymers (condensed tannins), Magn. Reson. Chem. 25 (1987) 118–124, https://doi.org/10.1002/MRC.1260250207.

[36] G. Jürgenliemk, F. Petereit, A. Nahrstedt, Flavan-3-ols and procyanidins from the bark of Salix purpurea L, Pharmazie 62 (2007) 231–234.

[37] O. Fritsche, Mikrobiologie, Springer Berlin Heidelberg, Berlin, Heidelberg, 2016.

[38] G. Semenza, S. Auricchio, N. Mantei, Small-intestinal disaccharidases, Online: https://ommbid.mhmedical.com/content.aspx?bookid=2709&sectionid=225081608.

[39] S. Jiang, J. Ghosh, Alpha glucosidase, RCSB PDB (2019), https://doi.org/10.2210/rcsb_pdb/GH/DM/drugs/gi/glucosidase.

[40] Y. Tsujimoto, H. Tanaka, R. Takemura, T. Yokogawa, A. Shimonaka, H. Matsui, S. Kashiwabara, K. Watanabe, Y. Suzuki, Molecular determinants of substrate recognition in thermostable alpha-glucosidases belonging to glycoside hydrolase family 13, J. Biochem. 142 (2007) 87–93, https://doi.org/10.1093/jb/mvm110.